Research Square

Preprints are preliminary reports that have not undergone peer review.
They should not be considered conclusive, used to inform clinical practice,
or referenced by the media as validated information.

Advanced Control Strategies for Continuous Flow Ohmic Heating: A Comparative Analysis of Conventional and Neural Network-Based Approaches for Sustainable Food Processing

Tasmiyah Javed
Sheffield Hallam University
Leo Pappukutty Luke
Sheffield Hallam University
Walid Issa
Sheffield Hallam University
James Spendlove
Sheffield Hallam University
Muhammad Akmal
Sheffield Hallam University
Timofei Breikin
Sheffield Hallam University
Caroline E Millman
Sheffield Hallam University
Mahdi Rashvand
Nottingham Trent University
Hongwei Zhang
H.Zhang@shu.ac.uk

Sheffield Hallam University

Research Article

Keywords: Continuous flow ohmic heating, Precise temperature control, Nonlinear dynamics, NN-based controllers, Performance comparison

Posted Date: April 8th, 2026

DOI: https://doi.org/10.21203/rs.3.rs-9252718/v1

License: This work is licensed under a Creative Commons Attribution 4.0 International License.
Read Full License

Additional Declarations: No competing interests reported.

Advanced Control Strategies for Continuous Flow Ohmic Heating: A Comparative Analysis of Conventional and Neural Network-Based Approaches for Sustainable Food Processing

T. Javed[1] · L.P. Luke[1] · W. Issa[2] · J. Spendlove[2] · M. Akmal[2] · T. Breikin[2] · C. Millman[1] · M. Rashvand[3] · H. Zhang[1]

Abstract: Continuous flow ohmic heating (CFOH) is a novel, energy-efficient, and sustainable food processing technique that employs the electrical resistance of food for rapid and uniform volumetric heating. The enhanced thermal efficiency and the absence of conventional coal or steam-based heating offer CFOH a feasible option for reducing greenhouse gas (GHG) emissions and advancing net-zero carbon objectives in industrial food processing. Precise temperature control is crucial, as fluctuations can compromise food quality, sensory attributes, and overall operational efficiency. The nonlinear dynamics of CFOH systems often challenge conventional proportional–integral–derivative (PID) controllers, requiring frequent tuning to maintain optimal performance. To overcome these limitations, advanced neural network (NN)-based control methods, proficient in managing nonlinear system dynamics by learning complex input-output relationships, can be utilised. In this research, NN-based control approaches, including nonlinear autoregressive moving average level 2 (NARMA-L2) and model reference control (MRC), are examined. This study performs a thorough performance comparison between traditional PID control and sophisticated neural network-based control methods, assessing their responsiveness, control precision, energy efficiency, and indirect greenhouse gas emission utilising a real-time validated physical model of a pilot-scale CFOH created in MATLAB/Simulink. The findings indicate that the NARMA-L2 controller outperforms both MRC and PID control, attaining a more rapid dynamic response, greater stability, superior energy efficiency without overshoot, and fewer GHG emissions. The MRC demonstrates moderate and consistent performance, while the PID has a slower response, significant overshoot, and elevated energy usage. Overall, NN-based control improves temperature regulation, lowers energy consumption, and promotes sustainable, low-carbon food processing systems.

Keywords: Continuous flow ohmic heating; Precise temperature control; Nonlinear dynamics; NN-based controllers; Performance comparison.

Introduction

The food and drink industry (FDI) is rapidly growing around the world and is forecasted to expand with a compound annual growth rate (CAGR) of 10.5% until 2029. In the United Kingdom (UK), it holds particular significance as the largest manufacturing sector, generating an annual turnover of £148 billion [1] massive industry carries a correspondingly large carbon footprint. Studies have revealed that the food processing system accounts for about 30% of total energy consumption and around 26% of all GHG emissions (as shown in Fig. 1), as the sector heavily relies on fossil fuels all over the world [2].

✉ H. Zhang
h.zhang@shu.ac.uk

1 Advanced Food Innovation Centre (AFIC), Sheffield Hallam University, Sheffield, United Kingdom

2 School of Engineering and Built Environment, Sheffield Hallam University. Sheffield, United Kingdom

3 Centre for Business and Industry Transformation, Nottingham Trent University, United Kingdom

In the UK alone, food and drink processing was estimated to consume about 24.6 TWh of energy and emit approximately 9.1 million tonnes of CO_2 per year [3].

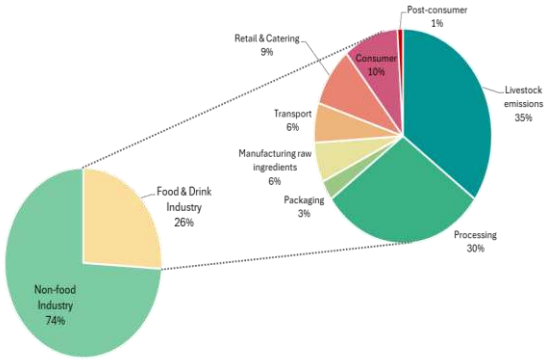


Fig. 1 Breakdown of GHG emissions in the UK Food & Drink Industry

The food processing industry is one of the major contributors to GHG emissions and industrial energy consumption. The sector's heavy reliance on conventional heating methods not only exacerbates environmental degradation but also places immense pressure on energy resources. In response, the UK's food and drink federation (FDF) has aimed to

achieve Net Zero emissions by 2040 [1]. This sector-wide target necessitates the widespread adoption of greener, more efficient processing technologies in food manufacturing. Consequently, considerable research is now focused on developing alternative and advanced technologies for sustainable food processing.

CFOH is an emerging industrial food processing technology characterised by direct volumetric heating, which reduces thermal losses and improves temperature uniformity. These characteristics improve process efficiency and reduce the carbon footprint by eliminating reliance on fossil fuel-based thermal energy, thereby establishing CFOH as a sustainable processing technology. However, the effective implementation of CFOH relies on intelligent control strategies and automation to balance operational stability, energy efficiency, and environmental impact. Such control approaches support industrial decarbonisation by reducing indirect greenhouse gas emissions associated with energy use. These assertions are supported by previous studies demonstrating that enhanced process control improves both control accuracy and overall system efficiency in nonlinear thermal systems [4].

Gethchell in the 1930s was among the first to stress the importance of controlling ohmic heating (OH) parameters [5].In those early implementations, control schemes were often rudimentary. Simple on/off thermostatic controllers were common in thermal systems because of their simplicity, but they led to oscillatory temperature swings and overshoot. Vandoren et al. (1998) noted that purely open-loop control of OH suffers from inaccuracy because the system cannot correct for disturbances or system errors [6]. Stirling et al. (1987) outlined the key control requirements for an ohmic heater, noting that the controller must maintain the outlet temperature despite variations in flow rate, incoming product temperature, and power input [7]. These early limitations underscored why more sophisticated control strategies became necessary as OH applications expanded.

By the late 20th century, researchers began introducing feedback control to OH systems to improve accuracy and robustness. During this period, a prevalent approach was the PID controller, which had become ubiquitous in industrial heating control. This is because it is straightforward to understand, easy to implement, and has satisfactory performance in linear or slowly changing systems. Numerous studies have been conducted on PID theory, tuning techniques, and practical applications in closed-loop systems. Research by Skudder et al. (1992) described an OH system where a microprocessor continuously adjusted electrical power based on feedback, comparing the desired output temperature with the measured output and modulating the transformer voltage accordingly [8]. This early PID-controlled ohmic heater marked a transition to closed-loop automation. Research by Li et al. (2019) demonstrated that basic temperature feedback, along with an integration of appropriate proportional control gain, can effectively regulate applied voltage in an ohmic heater, reducing steady-state error and improving stability [9]. Compared to on/off control, PID introduced smoother control action and reduced oscillations, but it still faced challenges with the intrinsic nonlinearity of OH. Temperature-dependent changes in the electrical conductivity of the product can significantly alter the dynamics of the system during operation, meaning that a fixed PID tuning may exhibit suboptimal performance in the presence of substantial nonlinearities and evolving operational parameters [10]. Hence, PID-controlled systems are optimised for a designated operating point and exhibit no adaptability to fluctuations in system performance.

Therefore, in systems such as CFOH that are characterised by significant nonlinearities, time-varying electrical characteristics, and interrelated thermal-electrical dynamics, the limitations of fixed-gain PID controllers become increasingly evident. Traditional controllers are unable to adapt to varying operational conditions, resulting in frequent temperature fluctuations, extended settling times, and increased energy use. This performance decline not only diminishes product quality and process safety but also undermines energy efficiency and the environmental advantages of sustainable thermal processing.

Consequently, researchers in thermal processing have observed these shortcomings and compared PID to more adaptive controls. A clear example is found in ohmic heating control experiments, where Dinc et al. (2024) designed both a PID and a fuzzy logic controller (FLC) for an OH system and compared their performance. The PID was tuned for optimal response at a given operating point, yet the FLC significantly outperformed it, achieving more stable temperature control, faster settling with no overshoot, and generally more powerful control action [11]. This indicates that the fixed-gain PID could not cope as well with the system's nonlinear behaviour, whereas the rule-based fuzzy controller could adapt its output to maintain stability. Such findings mirror results in other heating applications; for instance, fuzzy logic has also proven superior to PID in maintaining precise temperature on an induction-heating cooker, especially under varying conditions [12].

Likewise, conventional PID loops in milk pasteurisation units often struggle with the process's inherent time delays and time-varying dynamics, prompting the need for more advanced tuning or control schemes [13]. These examples underscore that if operating conditions are steady and well-characterised, PID control works, but in nonlinear,

time-varying environments typical of food processing, its performance and efficiency can be suboptimal. These issues emphasise the necessity of sophisticated control methodologies capable of learning system dynamics and adapting in real time to address nonlinear process behaviour. Recently, intelligent control methodologies employing artificial neural networks (ANNs) have garnered significant attention due to their capability to simulate intricate nonlinear systems without requiring explicit mathematical formulations. This enhances their robustness, adaptability, and precision in managing energy-intensive industrial operations [14].

Among these approaches, intelligent and nonlinear control systems, such as the NARMA-L2 controller, are designed to handle complex dynamics by eliminating inherent nonlinearities using trained models. In a variety of control systems, such as steel rolling mills, shell and tube heat exchangers, continuous stirred tank reactors (CSTRs), and chemical process models, the NARMA-L2 architecture has proven to be resilient to disturbances and to have better tracking performance than conventional controllers in nonlinear settings [15]-[17]. Using NN-based models of process dynamics, these controllers generate control actions that improve the linearity of the closed-loop behaviour. This facilitates quicker and less overshoot responses from highly dynamic systems. The enhanced control performance is particularly beneficial for CFOH systems, since faster and precise temperature regulation directly influences energy efficiency, operational stability, and the sustainability of the thermal processing operation.

Leveraging the advantages of intelligent nonlinear controllers, another formidable model-based control strategy for managing complex and nonlinear industrial processes is represented by MRCs. The closed loop's behaviour is precisely specified by MRC using a reference model. Rather than merely employing pre-established control heuristics, MRC techniques construct the controller so that the system's actual output corresponds to the response of a reference model, which illustrates the ideal behaviour of the system. By continuously adjusting the control action as necessary, MRC structures can improve tracking and disturbance rejection performance by comparing the plant output to the output of the reference model. Systems having dynamic uncertainties or nonlinearities are particularly affected by this. One prominent example is the reduction of power system oscillations using an NN-based MRC architecture. Reduced integral square error indices in simulation studies indicate that the MRC's model matching objective significantly enhances damping performance when compared to traditional proportional-integral (PI) control in this context [18]. Controller frameworks of this type demonstrate how model-referenced methods can maintain robust control over complex industrial processes while ensuring that the system's actual outputs meet the dynamic targets that were intended. In CFOH, the application of MRC techniques enhances temperature regulation, optimises energy efficiency, and amplifies the advantages of advanced control technology.

In the context of OH, adaptive controllers are highly beneficial because food properties (density, specific heat, conductivity) can change with temperature or as composition evolves (e.g., starch gelatinisation in a sauce). An adaptive algorithm can revise the control law on the fly to retain stability and performance despite these changes. However, ensuring stability during adaptation is a key challenge; the system must be carefully designed so that parameter updates improve performance without introducing oscillations. This often requires a robust estimation of the current system parameters, which itself can be sensitive to sensor noise or abrupt disturbances. Sensor inaccuracies pose a problem here: an adaptive controller updating its model based on noisy temperature readings might mistune itself. Thus, high-quality sensing and filtering are critical for successful adaptive control in ohmic heating. In the realm of OH, such hybrid and intelligent controllers are still an active research frontier, but their potential is clear.

Implementing advanced controllers enhances operational efficiency while simultaneously promoting environmental sustainability through improved energy utilisation. These intelligent control systems utilise reduced electricity, hence diminishing GHG emissions not directly attributable to them. This is particularly applicable in regions where fossil fuels are utilised for energy production. CFOH processes can maintain a consistent temperature and ensure the quality of items through appropriate control systems. This also assists enterprises in conserving funds while achieving their objectives for minimising their carbon impact and decarbonisation. Additionally, the capacity to dynamically optimise controller behaviour, as demonstrated by validated models and real-time CFOH pilot tests, highlights the growing importance of control engineering at the intersection of sustainability and industrial automation objectives [19]

Based on the reviewed literature, control strategies for ohmic heating systems and other thermal systems have evolved throughout time, from straightforward open-loop and on-off controls to traditional PID controls and, more recently, intelligent, adaptive, and hybrid control architectures. Although fixed-gain PID controllers are frequently employed in industry, they perform poorly in situations with numerous nonlinearities and fluctuating operational parameters. These

systems do not respond to shifts in system performance since they are tuned for a particular operating point [10]. Fuzzy logic and adaptive schemes are examples of intelligent controllers that have shown improved stability and robustness.

However, many existing approaches either focus primarily on temperature regulation without explicitly optimising dynamic performance metrics or impose significant design complexity and training dependencies. Further, while energy-efficient control is becoming increasingly popular, there are limited studies that systematically link improvements in controller performance to energy efficiency and the consequent drop in indirect greenhouse gas emissions associated with electrical energy use. Comparative studies evaluating both traditional and advanced intelligent controllers in a single framework for CFOH that consider control performance across several matrices and sustainability are conspicuously lacking. This disparity highlights how crucial it is to implement and evaluate novel control systems that can maintain precise temperature control while reducing response and settling times, overshoot, and control error. These developments are crucial for ensuring the safety and quality of food, but they are also crucial for improving energy efficiency and, eventually, reducing GHG emissions. These developments will increase the sustainability of thermal processing systems.

This study provides a comprehensive comparative analysis of conventional PID with advanced NN-based NARMA-L2 and MRC controllers, which are employed on a real-time validated physical model of a pilot-scale CFOH developed in MATLAB/Simulink, focusing on energy efficiency, system performance, and alignment of control strategies with sustainability standards. This study aims to provide empirical evidence on the importance of controller selection in improving eco-efficient industrial process control.

Experimental Configuration for Data Acquisition from Pilot-Scale CFOH

The pilot-scale CFOH is employed to gather data, with the working fluid in the system being a sweet and sour sauce exhibiting a conductivity of 0.6 S/m. A conductivity meter, the Apera Instruments Premium Series PC60 multiparameter pocket tester kit, was used for measuring conductivity. A pump connects the infeed tank to the ohmic heating chamber. The pump ensures continuous fluid flow into the heating chamber.

The ohmic chamber contains three vertically arranged electrodes 0.6 m and 0.8 m apart, encased in insulating layers. High voltage (HV) is applied to the central electrode, generating two heating zones: one between the infeed electrode and the central electrode (labelled as Electrode 2 in Fig. 2), and the other between the central electrode and the outfeed electrode. A thyristor operating in phase-angle control mode regulates the power delivered to the fluid by adjusting the voltage on the primary winding of the transformer. A programmable logic controller (PLC) governs this thyristor configuration; however, it can additionally be operated via Sheffield Hallam University's PC-based open-loop control system.

The chamber operates autonomously and is equipped with an integrated PLC-human machine interface (HMI) that enables the user to control the power supply. The system accommodates large power levels (up to 12 kW from a 63A supply) and a range of fluid conductivities (from 0.1 to 4 S/m), rendering it suitable for various food products. A crucial aspect of the system is its continuous monitoring of temperature across many locations. Thermocouple gauges assess the temperature of the infeed TC1 and the outfeed TC2. Fibre optic probes deliver precise temperature measurements. FT1 and FT2 monitor the exit temperature, whilst FT3 and FT4 assess the temperature within the heating chamber.

Activating the Pump Start button or executing the same action on the control PC will initiate the pump. The fluid is subsequently pumped upward, saturating the applicator beyond the outfeed electrode. The pump's speed can be adjusted as required. During operation, critical parameters such as voltage, current, power consumption, thermocouple measurements, fibre optic temperature readings, and flow rate are continuously monitored. The heating process finishes when the fluid exits the heating chamber and reaches the outfeed collection tank at the appropriate temperature.

Overall, the pilot-scale CFOH system is a highly regulated and adaptable platform for investigating thermal processes under real-time conditions. The system can precisely characterise heat transport and process dynamics due to its accurate power regulation, adaptable flow control, and multi-point temperature monitoring. This comprehensive experimental setup ensures accurate data gathering for the development of a more sophisticated data-driven neural network-based controller.

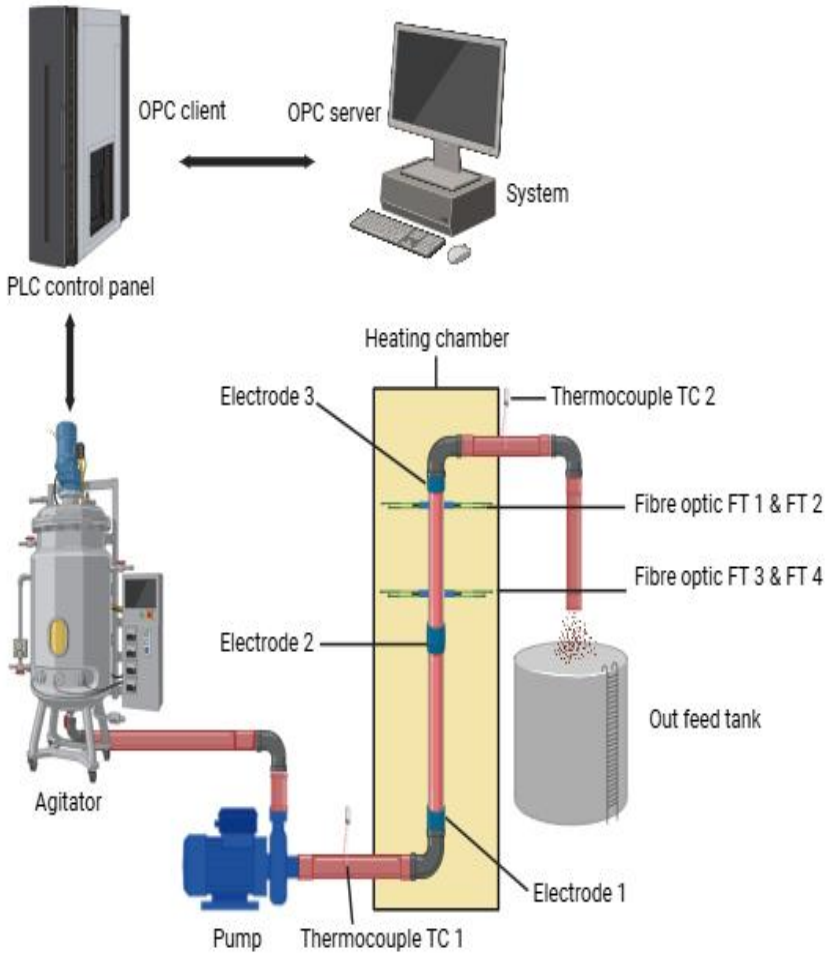


Fig. 2 Schematic diagram of a pilot-scale continuous flow ohmic heater

Open Platform Communications (OPC)-Based Communication Framework

Comprehensive data, including the entire operational process of the CFOH, has been collected for the training, testing, and validation of the NN-based controllers. Throughout the operation, critical parameters were continuously monitored and documented. An OPC server facilitated data collection by enabling the PLC managing the ohmic heater to communicate and exchange data with another computer in the laboratory. This configuration enabled the utilisation of both fundamental and intricate model-based control techniques within the MATLAB/SIMULINK framework.

The OPC server and client protocol provide real-time data transmission and reception over a local area network (LAN). The KEPServerEX OPC server was configured to communicate with the PLC via Ethernet using the PLC's Ethernet module. This configuration enables the lab PC to read from and write to the PLC, monitor data in real time, and store information. The technique enabled the utilisation of both basic and sophisticated controllers, facilitating precise operational control. The PLC transmitted input/output (I/O) tags to the OPC server, enabling MATLAB to communicate with the PLC for control and monitoring purposes.

Design of Proportional-Integral-Derivative (PID) Controller

The PID controller is a prevalent method for system regulation, integrating proportional, integral, and derivative actions to achieve desired system behaviour. The Ziegler–Nichols (ZN) tuning approach was employed to design and optimise a PID controller [24]. This method provides a framework for determining optimal controller settings based on the system's response to variations. The tuning procedure provided a proportional gain selection of $K_p = 1.6$, $K_i = 0.02$, and $K_d = 0$. The selected configurations ensure the system operates

efficiently, responds promptly, and maintains a minimal steady-state error for the specified setpoint. The calibrated PID controller serves as a standard for evaluating the dynamic responsiveness, energy consumption, and overall control efficiency of the neural-network controllers.

Design of Nonlinear Autoregressive Moving Average Level - 2 (NARMA-L2) controller for Continuous Flow Ohmic Heater (CFOH)

NARMA-L2 control and feedback linearisation are terms used to describe the NN controller discussed in this section. When the plant model has a particular form, it is called feedback linearisation (companion form). When the same form can be used to approximate the plant model, this is known as NARMA-L2 control. The main concept of this type of control is to cancel out the nonlinearities to convert nonlinear system dynamics into linear dynamics [20]. This section clarifies the companion form system concept and illustrates the application of an NN to identify this model. It subsequently clarifies the use of the identified NN model in the development of a controller. Fig. 3 depicts the working of the NARMA-L2 controller.

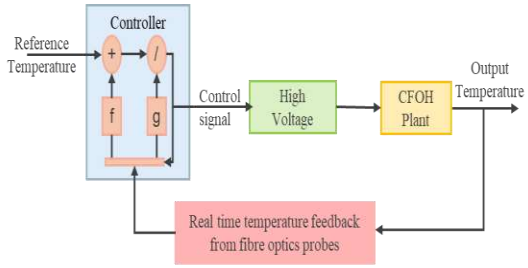


Fig. 3 Working of the NARMA-L2 controller

Identification of NARMA-L2 Model: The initial stage in employing feedback linearisation (or NARMA-L2) control is to identify the system designated for regulation. Train a neural network to model the forward dynamics of the system. The initial step is to select a model framework for implementation. The nonlinear autoregressive-moving average (NARMA) model is a typical representation for broad discrete-time nonlinear systems.

$$y(k+d) = N[y(k),y(k-1),\ldots,y(k-n+1),u(k),u(k-1),\ldots u(k-n+1)] \quad (1)$$

In the NARMA model, $y(k + d)$ denotes the expected output of the system d steps ahead; $y(k)$, $y(k - 1)$, …, $y(k - n + 1)$ represent the most recent n outputs reflecting the system's temporal evolution; and $u(k)$, $u(k - 1)$, …, $u(k - n + 1)$ comprise the current and preceding inputs influencing the system. The nonlinear function N maps these past inputs and outputs into the future output, where n denotes the model order, indicating the number of past steps considered.

To ensure the system output follows a reference trajectory, $y(k + d) = y_r(k + d)$, The subsequent step is to formulate a nonlinear controller with the following structure:

$$u(k) = G[y(k),y(k-1),\ldots,y(k-n+1),y_r(k+d),u(k-1),\ldots,u(k-m+1)] \quad (2)$$

The issue with employing this controller is that training a neural network to develop the function G for minimising mean square error necessitates the utilisation of dynamic backpropagation [21], [22]. This may be sluggish. A proposed approach by Narendra and Mukhopadhyay is the utilisation of approximate models to depict the system [23]. This part utilises a controller founded on the NARMA-L2 approximation model:

$$\hat{y}(k+d) = f[y(k), y(k-1),\ldots, y(k-n+1), u(k-1),\ldots, u(k-m+1)]+g[y(k),y(k-1),\ldots,y(k-n+1),u(k-1),\ldots, u(k-m+1)]\cdot u(k) \quad (3)$$

$y^{\wedge}(k + d)$ represents the expected system output d steps in advance. The expression $f[\cdot]$ denotes the nonlinear contribution of prior outputs y(k),…,y(k−n+1) and prior inputs u(k−1),…,u(k−m+1), which are independent of the current control, whereas $g[\cdot]$ is a nonlinear gain function that modulates the current input u(k) according to the same historical data. Together, $f[\cdot]$ and $g[\cdot]\cdot u(k)$ represents the discrete-time nonlinear dynamics of the system for predictive control.

This model is presented in companion form, wherein the subsequent controller input u(k) is excluded from the nonlinearity. This form allows for the determination of the control input that enables the system output to align with the reference y (k + d) = y_r (k + d). The resulting controller would have the form

$$u(k)= \frac{y_r(k+d)-f[y(k),y(k-1),\ldots,y(k-n+1),u(k-1),\ldots,u(k-n+1)}{g[y(k),y(k-1),..,y(k-n+1),u(k-1),\ldots,u(k-n+1)} \quad (4)$$

Employing this equation directly may lead to realisation issues, as it necessitates determining the control input u(k) concurrently with the output y(k). Therefore, utilise the model.

$$y(k+d)=f[y(k),y(k-1),\ldots,y(k-n+1),u(k),u(k-1),\ldots,u(k-n+1)]+g[y(k),\ldots,y(k-n+1),u(k),\ldots,u(k-n+1)]\cdot u(k+1) \quad (5)$$

where d ≥ 2. The Fig. 4 shows the structure of a neural network representation.

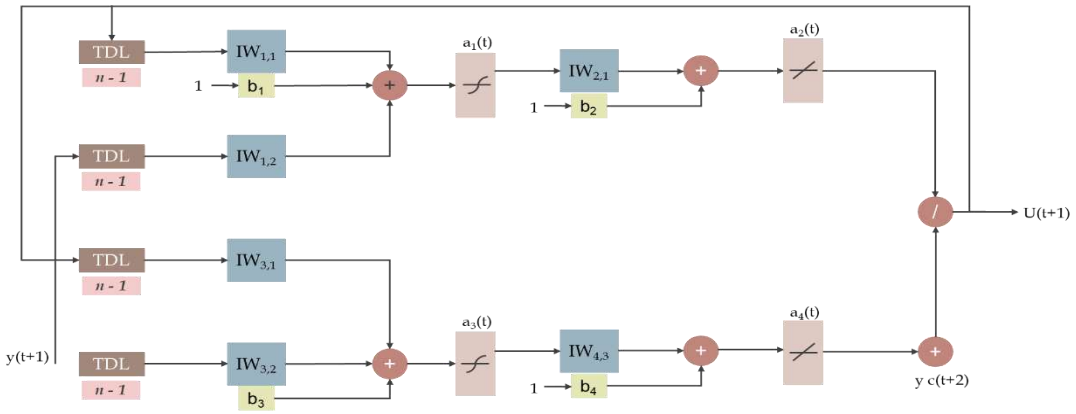


Fig. 4 Structure of neural network representation

NARMA - L2 Control law

The controller is obtained using the NARMA-L2 model

$$u(k+1)=\frac{y_r(k+d)-f[y(k),y(k-1),....,y(k-n+1),u(k-1),...,u(k-n+1)}{g[y(k),y(k-1),..,y(k-n+1),u(k-1),...,u(k-n+1)]} \quad (6)$$

which is realisable for d ≥ 2. Fig. 5 represents the block diagram of the NARMA-L2 controller.

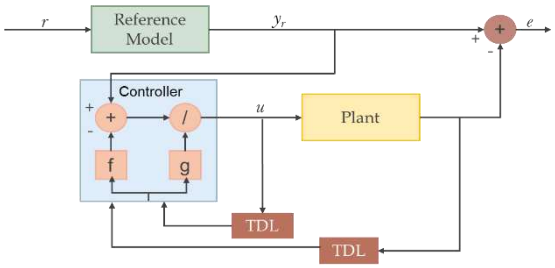


Fig. 5 Block diagram of NARMA-L2 Controller

The NARMA-L2 controller transforms a nonlinear plant into a linear system utilising an explicit control law derived from an affine neural model of the plant's dynamics. This approach presents the output of a nonlinear system as the aggregation of two functions, f [·] and g [·], identified by neural networks, with all nonlinearities distinct from the present control input [20]-[23]. The controller determines the subsequent control action by subtracting the anticipated nonlinear system behaviour from the desired future output. Subsequently, it amplifies the outcome by the estimated input gain. This mitigates the plant's nonlinearities and enforces linear input-output behaviour in the closed loop, enabling precise reference tracking. The controller may operate in real time and avoids being trapped in algebraic loops, as the control input is computed one step in advance (d≥2). This renders it ideal for rapid, nonlinear processes such as ohmic heating systems

Plant Identification of NARMA-L2 Controller

The collected experimental data were utilised to identify plants, a crucial stage in the development and testing of the controller. Consequently, the input and output variables were established. The voltage supplied to the system served as the input data, functioning as the thyristor set points. The output data utilised was the ultimate product temperature, designated as FT1, which is the fibre optic temperature sensor readings at the outlet. The identification approach utilised data points from the pilot–scale CFOH. This data was carefully chosen to include the entire range of CFOH operations. The created model effectively illustrates the temporal changes inside the system. This type of coverage is essential to ensure that the selected plant model is dependable and robust across many operational environments. Fig. 6 illustrates the process of plant identification by delineating the connections between inputs and outputs and constructing a plant model.

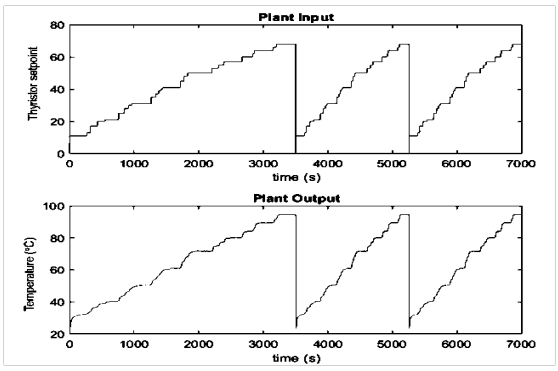


Fig. 6 Plant Identification of NARMA-L2 Controller

NARMA-L2 Neural network controller training, Testing, and validation

The subsequent phase involves training the neural network following the identification of the plant. The hyperparameters employed for training the NN were carefully chosen to optimise the performance (as shown in Fig. 7). The network was designed to capture the nonlinear relationships in the plant without overfitting, which was achieved by employing a hidden layer size of 13. The sampling interval was set at one second to ensure that the calculations could be performed swiftly while obtaining a comprehensive understanding of the system's operation. To ensure that the network accurately models the temporal dependencies in the NARMA-L2 system, it is crucial to consider the system's historical behaviour. Consequently, four delayed inputs and four delayed outputs from the plant were incorporated. The incorporation of four delayed inputs and four delayed outputs ensures that the neural network precisely replicates the primary dynamics and memory effects of the CFOH system. This selection achieves a compromise between model accuracy and computational efficiency, preventing both underfitting and excessive model complexity. The network was trained for 50 epochs using the Levenberg–Marquardt (LM) technique, which is highly effective for medium-sized networks and operates with speed and reliability. The neural network comprehends intricate relationships between the input and output data throughout the training phase.

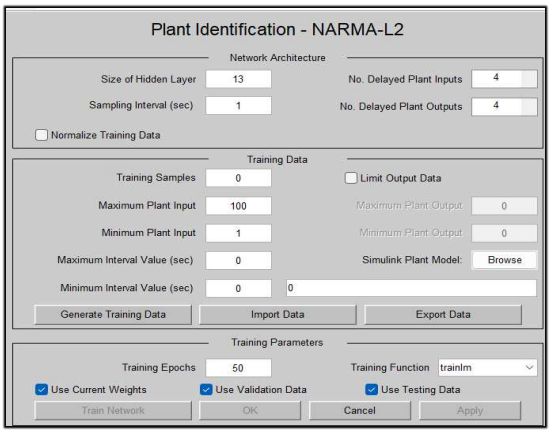


Fig. 7 NARMA-L2 Controller training parameters

Fig. 9 illustrates the utilisation of regression plots to evaluate the efficacy of the trained NARMA-L2 model across training, testing, and validation phases. The corresponding regression values are 0.99995, 0.99876, and 0.99893. The overall regression value is 0.99935. This regression data substantiates the correlation between neural network outputs and target values. The regression value, approximately equal to 1, indicates the strongest correlation.

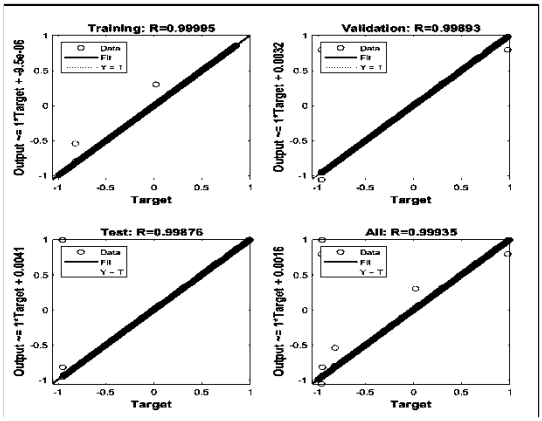


Fig. 9 NARMA-L2 regression plots

Design of an NN-based Model Reference Controller for Continuous Flow Ohmic Heater (CFOH)

MRC is a strategy where the desired behaviour of a system is defined by a reference model, and the controller is designed to make the actual plant output follow this reference model output. In essence, the controller continuously adjusts the plant input to minimise the error between the plant output and the reference model output. MRC typically consists of two main components: a reference model that encapsulates the ideal target dynamics and a control law (which can be fixed or adaptive) that drives the plant to emulate those dynamics.

In an MRC, learning algorithms are applied to achieve this goal. The general architecture uses two neural networks; one acts as a data-driven plant identifier, and the other is the controller. The neural network plant model is first trained to mimic the actual behaviour of the plant, and then the controller network is trained (using the plant model) so that the plant output tracks the reference model output. During operation, the controller takes the reference command and feedback signals to produce control actions that cause the real plant to follow the desired reference output. The block diagram of this illustration is shown in Fig. 10.

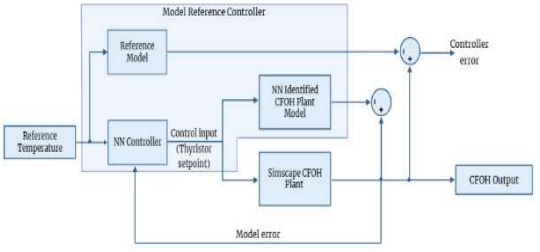


Fig. 10 Basic structure of Model Reference Controller (MRC)

In this architecture, the neural network controller has multiple inputs comprising delayed values of the reference input to account for reference changes over time, delayed values of the plant output, and delayed values of its past control

outputs. By including these delayed signals, the controller network can infer the system's state and history, which is crucial for controlling dynamic systems. The neural network plant model is usually a NARX-type network (Nonlinear Autoregressive with Exogenous input) that takes inputs as the delayed control inputs (plant inputs) and delayed plant outputs, and outputs the predicted next plant output. This plant model network captures the plant's dynamics. The number of delay terms (past time steps) is chosen based on the system's order or memory.

Plant Identification of Model Reference Controller

Before designing the controller, it is critical to obtain an accurate data-driven model of the plant. In this research, the plant identification was conducted using sweet and sour sauce as the product fluid, with an initial electrical conductivity of 0.6 S/m and a flow rate of 1 L/min (these conditions provide a consistent baseline for modelling). The input-output data for the plant identification process is shown in Fig. 11. The network architecture for this process was chosen using a grid search method, where the hyperparameters of the NARX network were tuned repeatedly until the target performance of the network model was achieved. The architecture of this model is shown in Fig. 12

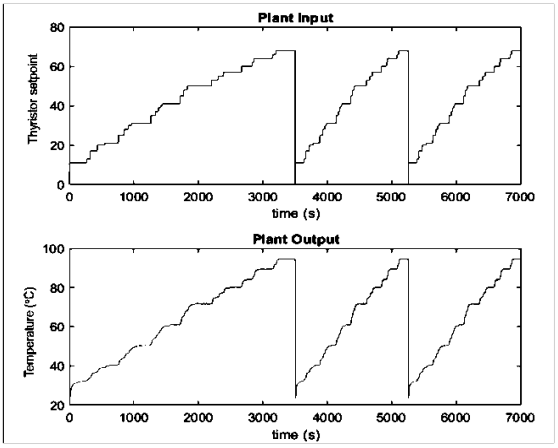


Fig. 11 Input-output data for plant identification

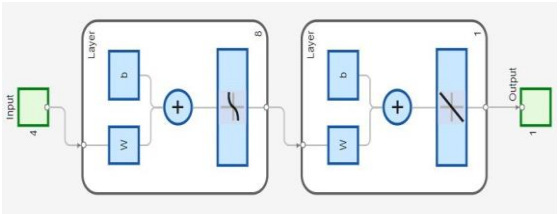


Fig. 12 Neural network architecture for plant identification

Key hyperparameters for plant identification are:

Network architecture

2-layer feedforward (NARX) network with 9 neurons in the hidden layer. A single hidden layer with 9 neurons was found sufficient to capture the plant's non-linear behaviour without overfitting. This was empirically determined; 9 neurons gave good performance for the CFOH plant.

Delayed inputs/outputs

The network was configured with 2 delayed plant inputs and 2 delayed plant outputs. This means the plant model considers the last 2 time-step values of the input (thyristor setpoint) and output (temperature) when predicting the next output. Using 2 delays allows the network to model up to second-order dynamics of the heater, which was appropriate given the thermal inertia and transport delays in the system.

Sampling interval

Data was sampled every 1 second during identification. This interval is aligned with the real-time data collected from the pilot plant. It is short enough to capture the significant dynamics of the thermal process.

Input range

The plant input (thyristor power setpoint) was varied over a range of 1 to 100% during identification. This corresponds to the minimum and maximum CFOH power settings. The output temperature corresponding to this input range spanned roughly from the inlet temperature (16 °C) up to near the maximum desired temperature (100°C).

Training algorithm

Levenberg–Marquardt backpropagation (Trainlm) was used for training the neural network plant model. Trainlm is a fast, second-order optimisation method well-suited for moderate-sized networks, and it typically converges in relatively few epochs for function approximation tasks. In this design, 150 training epochs were chosen as an optimal balance between sufficient learning and the prevention of overfitting. Using trainlm, the network training converged to a mean squared error (MSE) of 0.0023 and an overall regression (R) value of 0.998 (as shown in Fig.13), indicating that an accurate model of the plant was achieved.

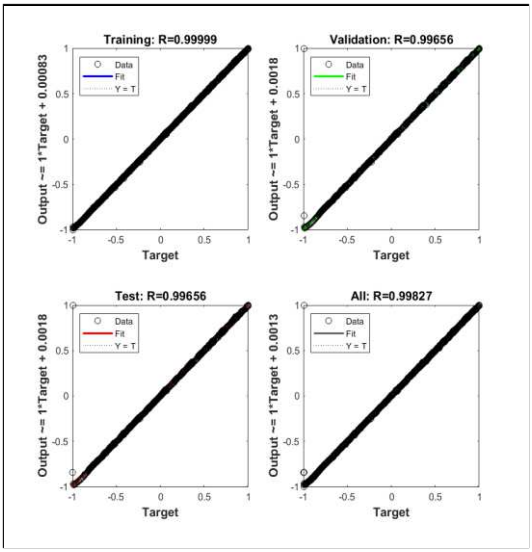


Fig. 13 Regression plot for plant identification

The outcome of the plant identification was a neural network model that predicts the outlet temperature of the saline solution given the current and recent past values of the thyristor input and temperature. The accuracy of the model was validated by comparing its predictions to actual plant data not seen in training, shown in Fig. 14. As the CFOH process can be non-linear, the neural network approach is advantageous; it can capture these non-linear relationships where a simple linear model would falter. A well-trained plant model is crucial for accurate predictions for the controller to operate efficiently in the defined range of control operation.

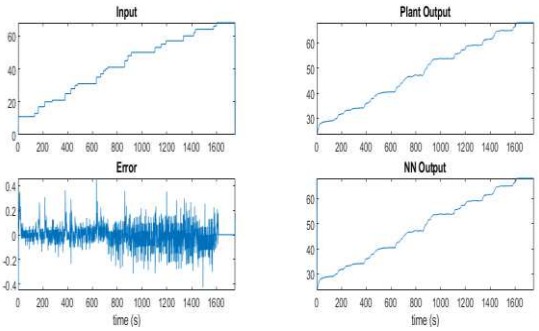


Fig. 14 Real-time plant output and NN-based plant identification output for test data

Model Reference Controller Training

After an accurate plant model, the next step was to design the MRC. The control goal is to make the outlet product temperature track a desired temperature trajectory, provided by the reference model, despite disturbances or non-linearities. The design and training of the controller were also carried out in MATLAB/Simulink using the MRC block. The reference model used the state-space model defined in equations 7 and 8.

$$x\ (k\ +\ 1)\ =\ Ax(k)\ +\ B_u u(k)\ +\ B_v v(k)\ +\ B_d d(k)) \quad (7)$$

$$y(k)\ =\ Cx(k)\ +\ D_y v(k)\ +\ D_d d(k) \quad (8)$$

where k is the time step index. In this model, x ∈ ℜn is the state vector representing the system's temperature states, u is the control input (the voltage input to the ohmic heater), and y is the controlled output (the product temperature). The terms v and d represent measured and unmeasured disturbances, respectively. For example, v could include mass flow rate or inlet temperature measurements if they were varying, while d might accumulate unmeasured effects like ambient losses or modelling error. The matrices A, B_u, B_v, B_d, C, D_y, and D_d define the dynamic relationships between these variables. This state-space formulation can accommodate time-varying parameters; however, a conventional MPC assumes these matrices remain fixed around a nominal operating point, implying that it is a linearised steady-state model.

For the CFOH system in this research, a linearised state-space model was obtained around the normal operating conditions. The model has two states (x = 2), which capture the thermal dynamics of the continuous flow ohmic heater. The specific state matrices at the nominal point are given below.

$$A = \begin{bmatrix} 0.997 & 0.296 \\ -7.19 \times 10^{-4} & 0.969 \end{bmatrix} \quad (9)$$

$$B_u = \begin{bmatrix} 8.3 \times 10^{-5} \\ 5.5 \times 10^{-4} \end{bmatrix} \quad (10)$$

$$C = \begin{bmatrix} h & i \\ 1 & 0 \end{bmatrix} \quad (11)$$

The state matrix A indicates that the first state (product temperature) tends to persist with a factor of 0.997 each step (very slow decay, effectively near integrator), and it is coupled to the second state with the 0.296 term. The second state (representing thermal accumulation in the heating chamber) also has a high factor of 0.970 and a small coupling back to the first state, -7.19×10^{-4}. Overall, the eigenvalues of A are close to 1, reflecting the slow dynamics and strong thermal inertia of the system.
The input matrix Bu represents changes in the manipulated variable (voltage input), u(k), that have a direct, though small, effect on both states. Notably, the second state has a larger gain (5.5×10^{-4}) from the input than the first state (8.3×10^{-5}), suggesting the input initially influences an internal energy state which then drives the output state. For this model, we did not include any measured disturbance inputs, so $B_v = 0$. Likewise, there were no direct unmeasured disturbance influences on the state equation, so $B_d = 0$.

The output matrix C means the controlled output y is taken to be the first state directly. In this

case, that first state corresponds to the outlet fluid temperature. The second state is not directly measured as an output, but it influences the first state through the dynamics in matrix A. The contribution of the second state to the first output is weighted by i. The terms $D_y = 0$ and $D_d = 3.3 \times 10^{-4}$ have no direct feedthrough from any measured disturbance to the output. However, a small constant term $D_d = 3.3 \times 10^{-4}$provides a bias on the output from unmeasured disturbances. The value is very small; it can account for a slight offset in temperature that is captured by the states. This helps the controllers to eliminate steady-state error by accounting for the fact that a tiny constant input might be needed to maintain temperature (example, compensating for heat losses).

The NN controller is a two-layer network (one hidden layer) with the following configuration:

Hidden layer size:

35 neurons were used in the hidden layer. This relatively large number of hidden neurons gives the controller enough capacity to represent the complex mapping from inputs (reference and feedback history) to the output (control action). We empirically arrived at 35 by increasing the hidden units until the controller's training performance stopped noticeably improving—fewer neurons led to high tracking error, while a higher number of neurons did not yield much better performance but would risk overfitting or slower training.

Controller inputs (delays)

The controller was provided with two delayed reference inputs, two delayed plant outputs, and two delayed controller outputs. In total, that means at each time step the controller sees the current reference r(t) and one past value r(t − Δt); the last two measurements of the plant output (temperature) y(t), y(t − Δt); and the last two control signals it generated u(t − Δt), u(t − 2Δt). Here, Δt represents the sampling interval of the discrete-time system. These inputs give the controller a memory of what has recently happened. Including delayed plant outputs helps the controller account for the plant's inertia and trend (e.g., is temperature rising or falling), and including delayed controller outputs (past actions) helps it understand how its previous actions are still affecting the plant (since the plant has memory). The two delayed reference inputs allow the controller to anticipate changes; if the reference is going to or has just changed, the controller can begin to respond proactively. This structure (with multiple delays) is a standard design in model-reference neural controllers.

Controller output

The output of the controller network is the manipulated variable for the plant, in the case of this research, the thyristor setpoint. The controller's task is to output the correct power level u(t) such that the plant's temperature reaches the desired value. The output has been constrained within the allowable range of the actuator: 1 to 100.

Training method

The controller network is trained with the plant model in the loop using dynamic backpropagation across time. A sequence of reference inputs is generated, the closed-loop simulation with the plant model is executed to obtain the plant output, the error relative to the reference model output is computed, and subsequently, the controller weights are adjusted to minimise this error. This process effectively requires backpropagating the error through the plant model and controller over time since the controller's current action affects future errors. The controller network was trained for 120 epochs to provide sufficient weight convergence without overfitting. It is noteworthy that the time required for each controller training cycle is almost twice that of plant model training, due to the need for dynamic backpropagation through sequences. Each training iteration must simulate the plant model forward in time and propagate errors backwards through time, which is computationally intensive.

After completing the training process, the NN controller was configured with the final optimised weights. To assess its performance, the NN output was compared against the corresponding output of the plant model (the results are displayed in Fig. 15). This comparison demonstrated that the controller was capable of accurately tracking the reference model.

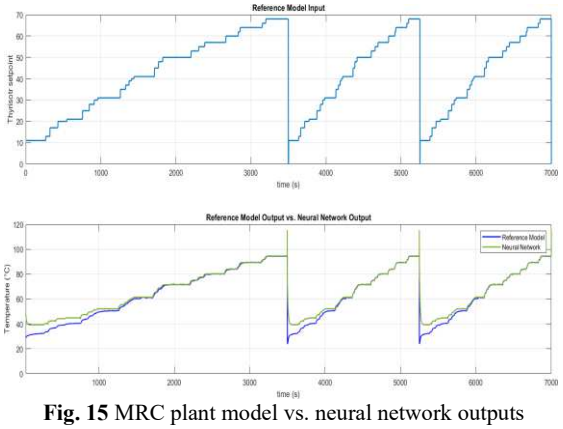


Fig. 15 MRC plant model vs. neural network outputs

Implementation of the developed controllers in a physical model of the CFOH in the MATLAB/Simulink environment

Employing a validated physical model provides a secure, adaptable, and energy-efficient method for testing controllers while maintaining a near approximation to the actual process. A physical model (often implemented in a simulation environment) aims to represent the actual system's behaviour more realistically by incorporating true multiphysics interactions. Unlike a highly simplified transfer function, a physical model can include nonlinear relationships and directly utilise physical laws, often resulting in improved accuracy. Indeed, physical models are better at capturing complex and dynamic behaviours, such as the coupling between electrical and thermal fields and the feedback of temperature on electrical conductivity, that might be challenging to express with linear equations.

Additionally, a physical model can be interfaced with real-time data: sensor measurements from an operating system can be fed into the model to update its states, effectively creating a digital twin of the process. This capability opens the door to advanced applications like predictive monitoring, fault detection, and model-based control, where the model runs in parallel with the actual process and helps adjust inputs continuously. In this study, a high-fidelity, real-time, validated physical model of CFOH (shown in Fig. 16) is used for testing developed control strategies and optimising performance without risking actual product or equipment [24].

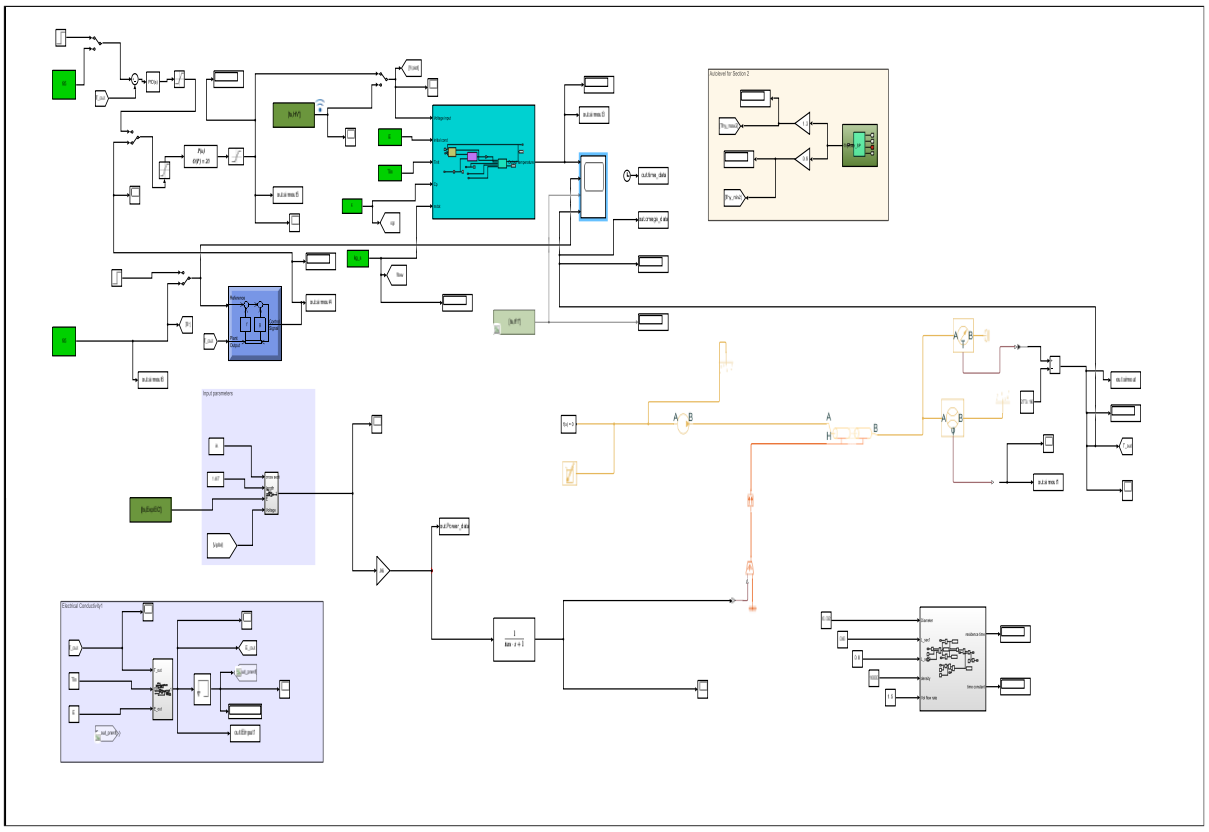


Fig. 16 Real-time validated CFOH Simulink physical model

Results & Discussion: Performance Analysis of the Controllers

Setpoint Tracking

NARMA-L2, MRC, and PID controllers were deployed in a MATLAB simulation using the real-time validated CFOH plant model developed and published in [24]. The properties of the sample product used in the simulation were of a proprietary sweet & sour sauce from a local industry. The product enters at an initial temperature of 16 °C with an electrical conductivity of 0.60 S/m. The controllers were tasked to heat the product to a setpoint of 95°C, reflecting a typical pasteurisation target. Fig. 17 shows the performance of each controller for the specified target temperature.

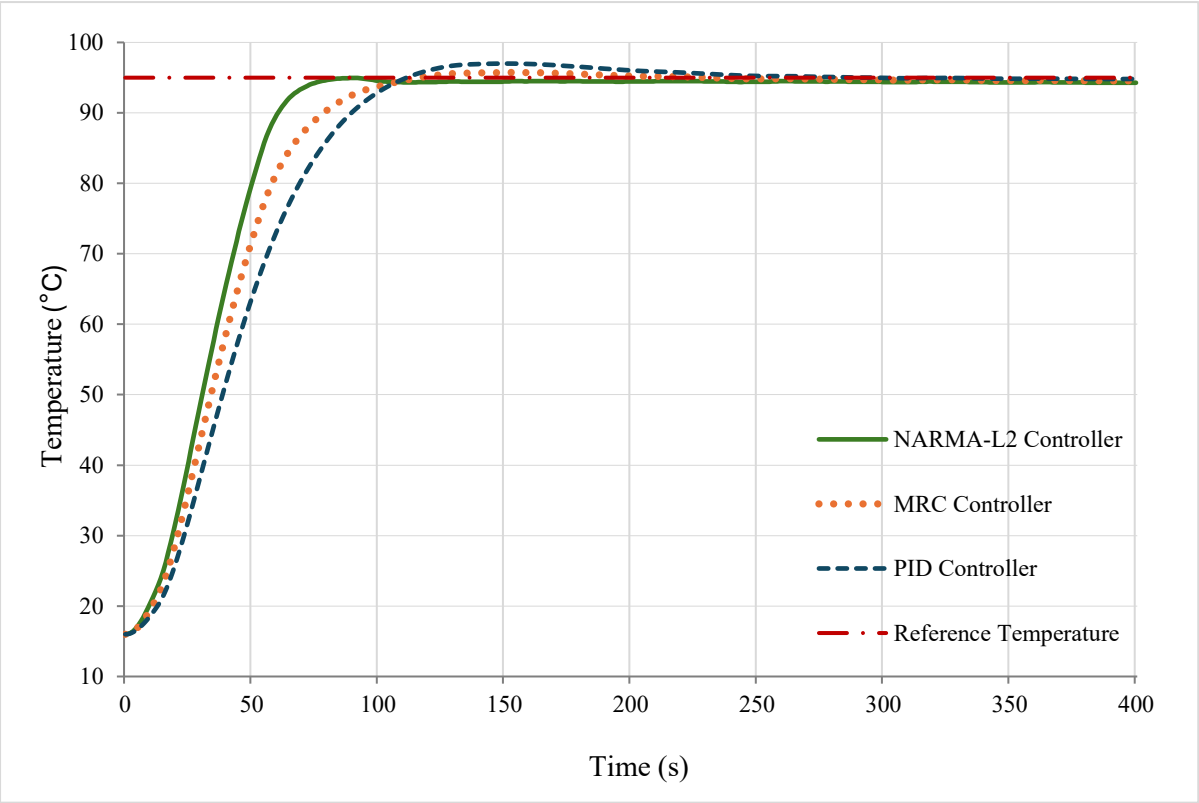


Fig. 17 Response of NARMA-L2, MRC, and PID controllers in simulation for sweet and sour sauce from 16 °C to 95 °C with initial conductivity 0.6 S/m

Performance Metrics

The effectiveness of the designed controllers in sustaining the target temperature of 95° C is assessed by several performance metrics. The comparative dynamic performance analysis demonstrates that neural network-based controllers consistently outperform classical PID controllers across all transient response metrics. The NARMA-L2 controller exhibits a rise time of merely 54.76 seconds, which is approximately 17.8% faster than the MRC (66.58 s) and 30.4% faster than the PID controller (78.64 s), as illustrated in Table 1. It demonstrates the high responsiveness of the NARMA-L2 controller. The NARMA-L2 controller exhibits a reduced rise time, enabling it to rapidly achieve the desired temperature more effectively than other controllers.

The transient time, defined as the duration required for the system to recover and stabilise following a significant change, was shortest for the NARMA-L2 controller at 69.74 seconds. The MRC controller required 96.51 seconds, but the PID controller necessitated 177.95 seconds. The abbreviated transient phase indicates that the NARMA-L2 and MRC controllers are more effective in mitigating prolonged oscillatory behaviour and accelerating the transition to steady-state operation. The settling time further illustrates the efficacy of advanced control strategies.

The settling time, which indicates the time required for the system's response to remain within a specified tolerance band around the setpoint, was significantly decreased under NARMA-L2 control, achieving steady-state conditions in 68.31 seconds. The MRC required 93.69 seconds, whilst the PID controller took far longer, at 163.23 seconds, to stabilise. This demonstrates that the NARMA-L2 and MRC enhance convergence speed and improve closed-loop stability.

The NARMA-L2 controller demonstrated superior performance regarding overshoot by maintaining the system output within the specified temperature limits. The MRC experienced a slight overshoot of 0.78%, whereas the PID controller exhibited a more substantial overshoot of 2.10%. None of the controllers induced undershoots, which is significant as it indicates that the system response did not fall below the setpoint during transient operation. These results indicate that the NARMA-L2 controller exhibits superior dynamic performance, characterised by a more rapid reaction, reduced oscillations, and enhanced stability. This renders it particularly effective for accurate and energy-efficient temperature regulation in CFOH. The MRC controller exhibits moderate performance with an acceptable overshoot. The PID's performance is inferior regarding responsiveness and overshoot.

Table 1 Performance analysis of NARMA-L2, MRC, and PID controllers for sweet & sour sauce heating from 16 °C to 95 °C with 0.6 S/m conductivity

Performance Metric	NARMA-L2 Controller	MRC Controller	PID Controller	Improvement of NARMA-L2 vs PID (%)	Improvement of MRC vs PID (%)
Rise Time (s)	54.76	66.58	78.64	30.36	15.34
Transient Time (s)	69.74	96.51	177.95	60.81	45.77
Settling Time (s)	68.31	93.69	163.23	58.15	42.60
Overshoot (%)	0.00	0.78	2.10	100	62.86
Undershoot (%)	0.00	0.00	0.00	-	-

Energy Efficiency and Power Consumption Analysis

The comparative examination of the NARMA-L2, MRC, and PID controllers during the simulation period reveals significant disparities in both the transient (1–70 s) and steady-state (71–400 s) phases, as illustrated in Table 2. The initial delay of around 15 seconds in the power and efficiency profiles is mostly attributed to inherent process dynamics, including thermal inertia, temperature-dependent electrical conductivity, and fluid residence time. Minor contributions arise from sensor latency and controller initialisation. The subsequent rapid rise in power results from the nonlinear enhancement of electrical conductivity and the efficient utilisation of the controller.

During the transient phase, NARMA-L2 has the highest average power consumption at 6043.58 W, followed by MRC at 5508.40 W and PID at 4973.23 W. Thus, the energy consumption at this period is highest for NARMA-L2 (0.1191 kWh), indicating its more robust reaction to initial system changes. In contrast, the PID controller, while showing the minimal energy consumption in this phase (0.0980 kWh), also reveals the lowest efficiency (29.04%), signifying its inadequacy in converting input energy into the necessary control action during the transient period.

The MRC demonstrates a balance between moderate energy consumption (0.1086 kWh) and relatively high efficiency (36.21%), highlighting its capacity to efficiently regulate system dynamics while maintaining optimal energy utilisation. The power consumption and energy efficiency are shown in Fig. 18 and Fig. 19.

In the steady-state phase (71–400 s), all controllers achieve similar average power levels, with PID (5317.37 W) slightly surpassing MRC (5259.88 W) and NARMA-L2 (5202.39 W). Regarding the energy consumption, PID consumes 0.4874 kWh, marginally higher than MRC (0.4822 kWh) and NARMA-L2 (0.4769 kWh). Despite slight fluctuations in power, the efficiencies of all controllers remain high, exceeding 91%, indicating effective energy utilisation during steady-state operation. NARMA-L2 has optimal efficiency (92.996%) in this phase, signifying a strong ability to maintain system operation with minimal energy consumption. This result demonstrates that the selection of a controller should consider the trade-off between long-term energy efficiency and rapid transient reaction. NARMA-L2 is the superior choice for steady-state efficiency and faster response, while MRC is an excellent option for overall balanced performance (as shown in Fig. 20).

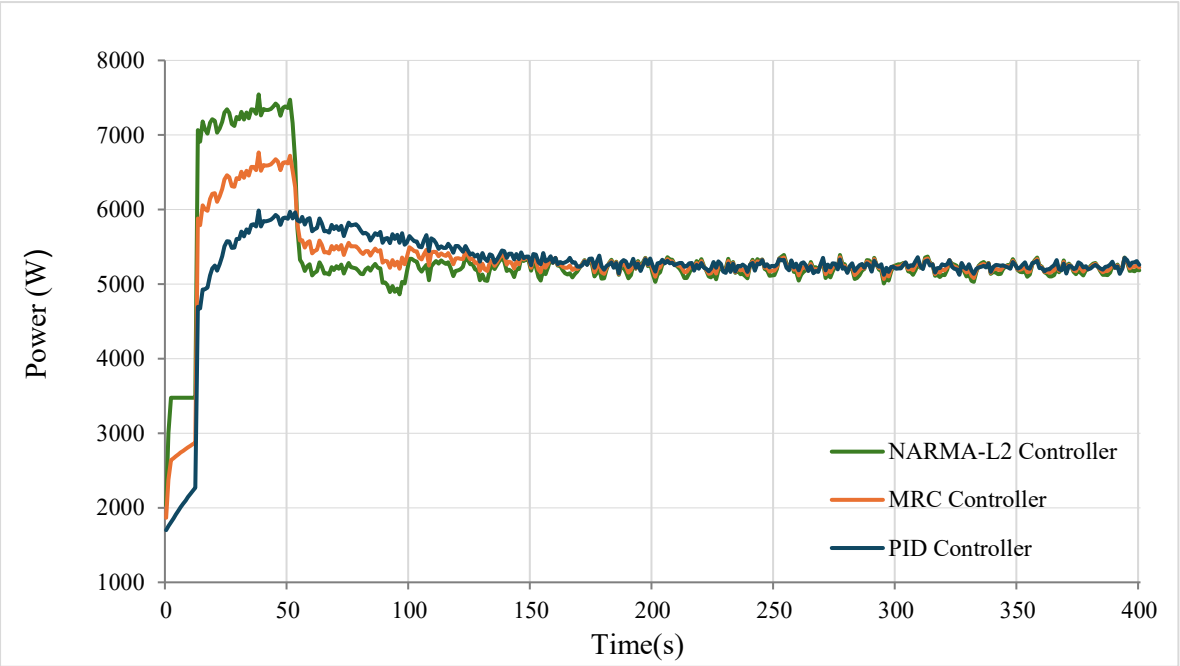


Fig. 18 Power consumption comparison by NARMA-L2, MRC, and PID controllers for heating sweet and sour sauce from 16 °C to 95 °C with electrical conductivity of 0.6 S/m

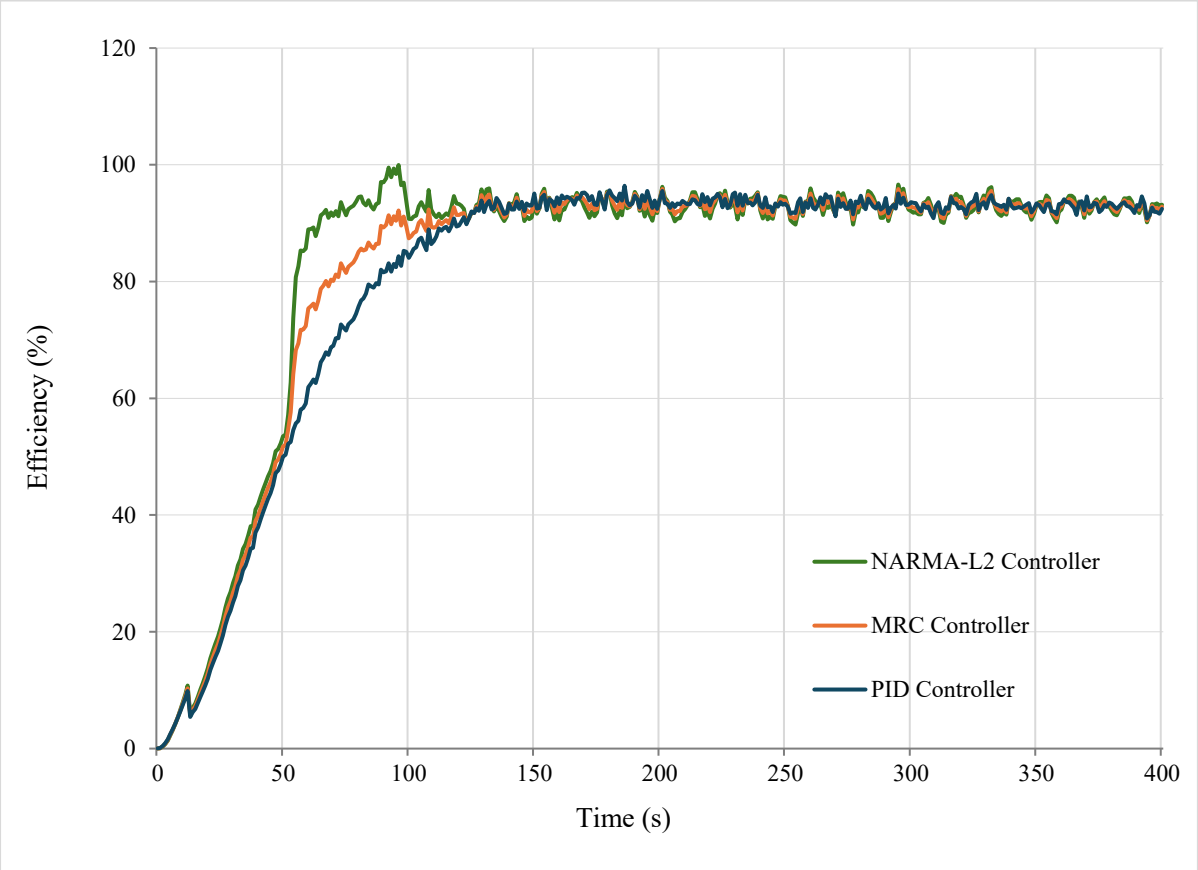


Fig. 19 Energy efficiency comparison by NARMA-L2, MRC, and PID controllers for heating sweet and sour sauce from 16 °C to 95 °C with electrical conductivity of 0.6 S/m

Table 2 Power consumption and energy efficiency comparison of the NARMA-L2, MRC, and the PID controllers for heating sweet and sour sauce from 16 °C to 95 °C with an electrical conductivity of 0.6 S/m

Controller	Average power (W)		Energy (kWh)		Efficiency (%)	
	1 - 70 s	71 - 400 s	1 - 70 s	71 – 400 s	1-70 s	71-400 s
NARMA-L2	6043.58	5202.39	0.1191	0.4769	35.37	92.99
MRC	5508.40	5259.88	0.1086	0.4822	36.21	92.28
PID	4973.23	5317.37	0.0980	0.4874	29.04	91.55

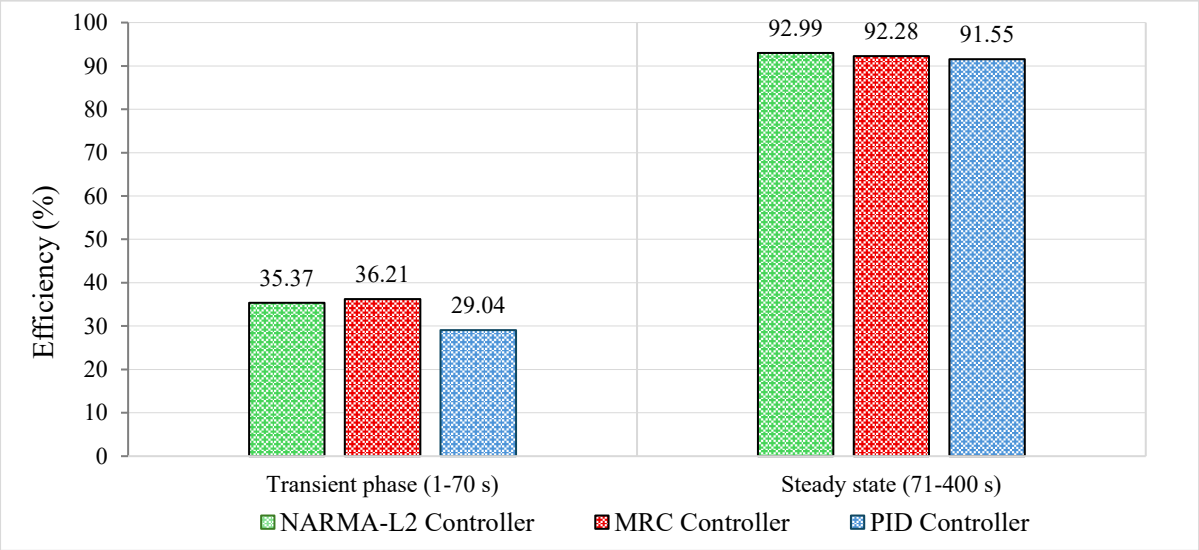


Fig. 20 Energy efficiency comparison of NARMA-L2, MRC, and PID controllers at transient and steady state for heating sweet and sour sauce from 16 °C to 95 °C with 0.6 S/m conductivity

Robustness Analysis of the Controllers

In addition to the above pasteurisation scenarios, robustness tests were conducted in simulation for all three controllers. The CFOH model was subjected to variations in the sweet & sour sauce initial electrical conductivity and step changes in the target temperature setpoint to rigorously challenge each controller's ability to handle variability.

Controllers' robustness with different initial conductivity

The electrical conductivity of real food products can vary between batches or over the course of heating. To simulate this, the model was given scenarios where the initial conductivity of the sauce was offset from 0.60 S/m, i.e., a low-conductivity case at 0.50 S/m and a high-conductivity case at 0.70 S/m, representing about ±16.7% variation. The controllers were not retuned for these cases, so this tested their resilience to modelling error. In the robustness evaluation, all three controllers (NARMA-L2, MRC, and PID) maintained similar temperature response characteristics, as shown in Fig. 21 and Fig. 22. The transient response (e.g., rise and settling times) remained largely consistent across these conductivity values, with only minor timing differences, at most about 2 to 3 seconds variation in settling time around the 0.6 S/m case. This indicates that each controller effectively handled the change in conductivity without significant performance degradation, which is an indication of their robust designs.

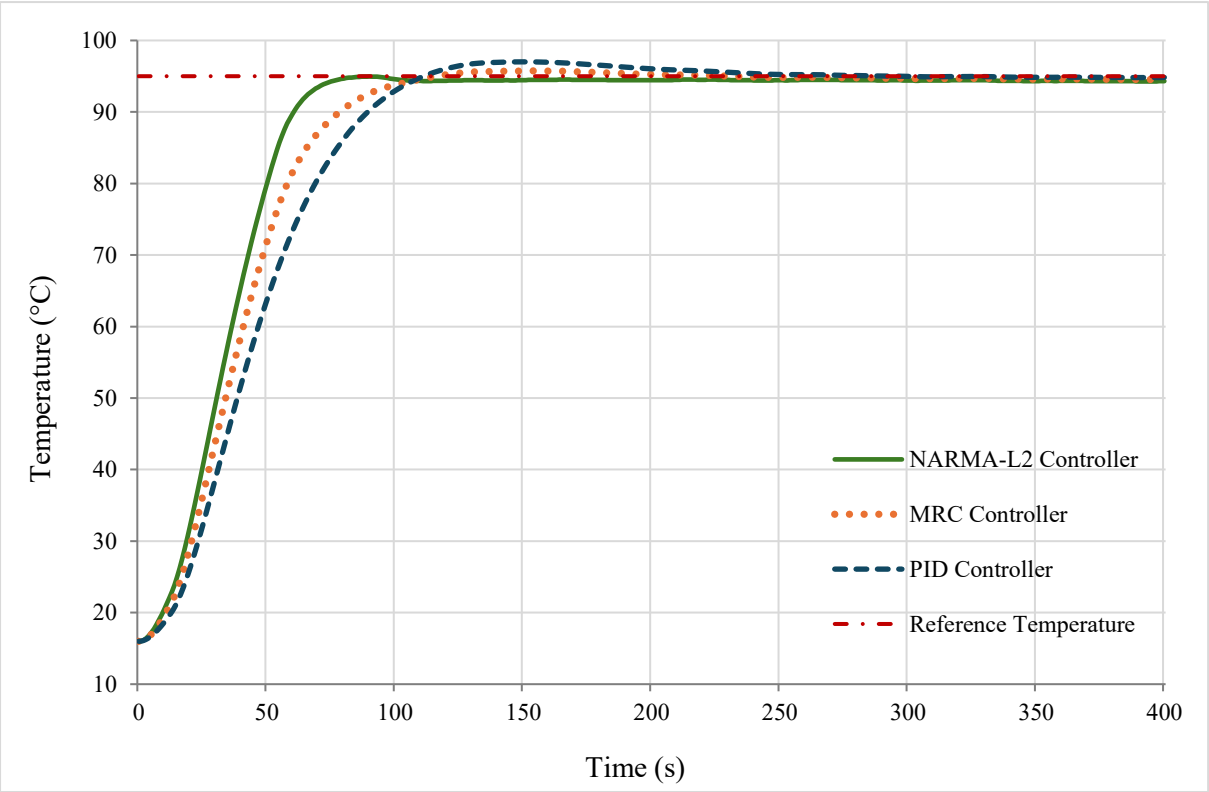


Fig. 21 Temperature response of NARMA-L2, MRC, and PID controllers in simulation for Sweet and Sour Sauce with initial conductivity = 0.50 S/m

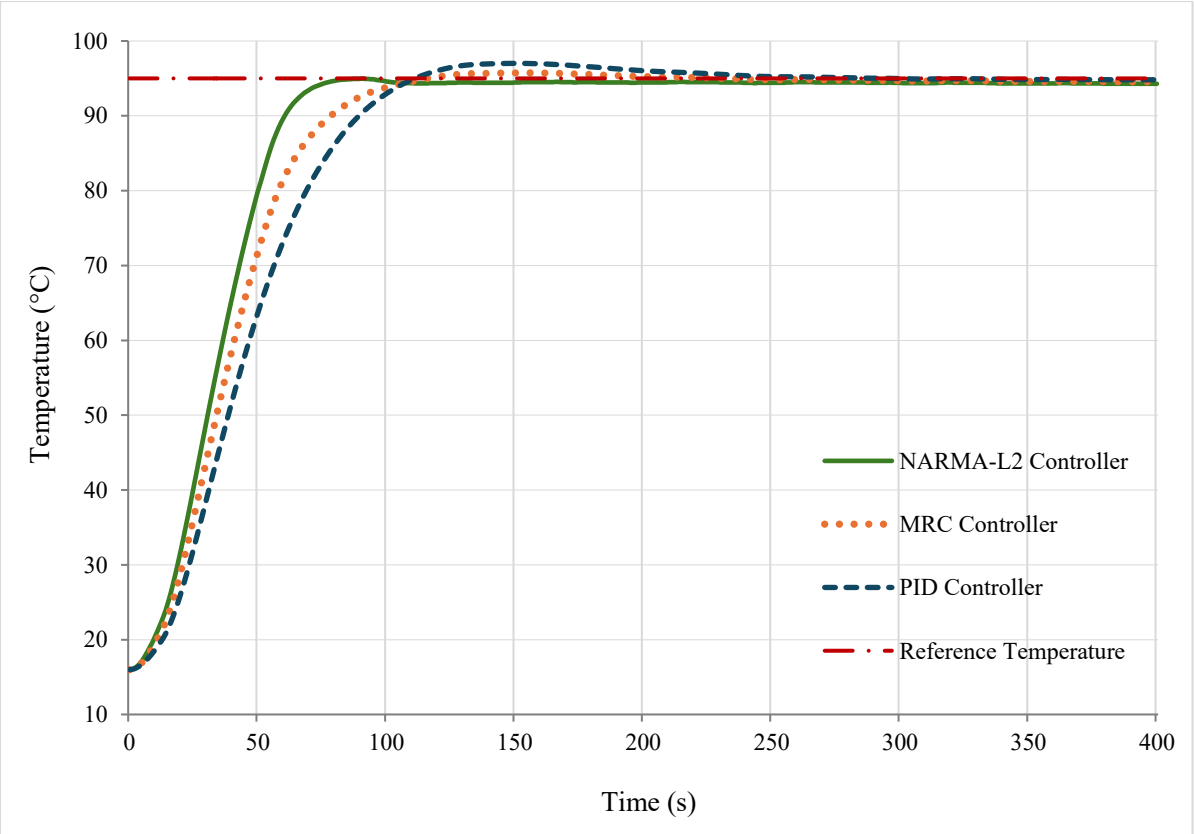


Fig. 22 Temperature response of NARMA-L2, MRC, and PID controllers in simulation for Sweet and Sour Sauce with initial conductivity = 0.70 S/m

Controller robustness under varying setpoint conditions

The other important robustness test for control systems involves assessing their response to sudden setpoint changes, which directly challenges the ability of the controller to handle large disturbances while maintaining stability, accuracy, and efficiency. In the context of continuous flow ohmic heating, where temperature must be precisely regulated in the presence of unpredictable input fluctuations, e.g., in food composition, flow rate, or desired product profile, the ability to adapt rapidly to such changes becomes essential.

To evaluate this, a step change in the reference temperature was introduced, which was from an initial steady state of approximately 50 °C to a high final setpoint of 95 °C at 250 seconds into the test sequence. The resulting temperature responses under NARMA-L2, MRC, and PID controllers are presented in Fig 23. The results reveal that all three controllers accurately tracked the change in temperature setpoints. The NARMA-L2 controller is the fastest to reach the setpoint, followed by the MRC and then the PID controller. This performance demonstrates that neural network-based controllers are more resilient and responsive to changes than a conventional PID controller.

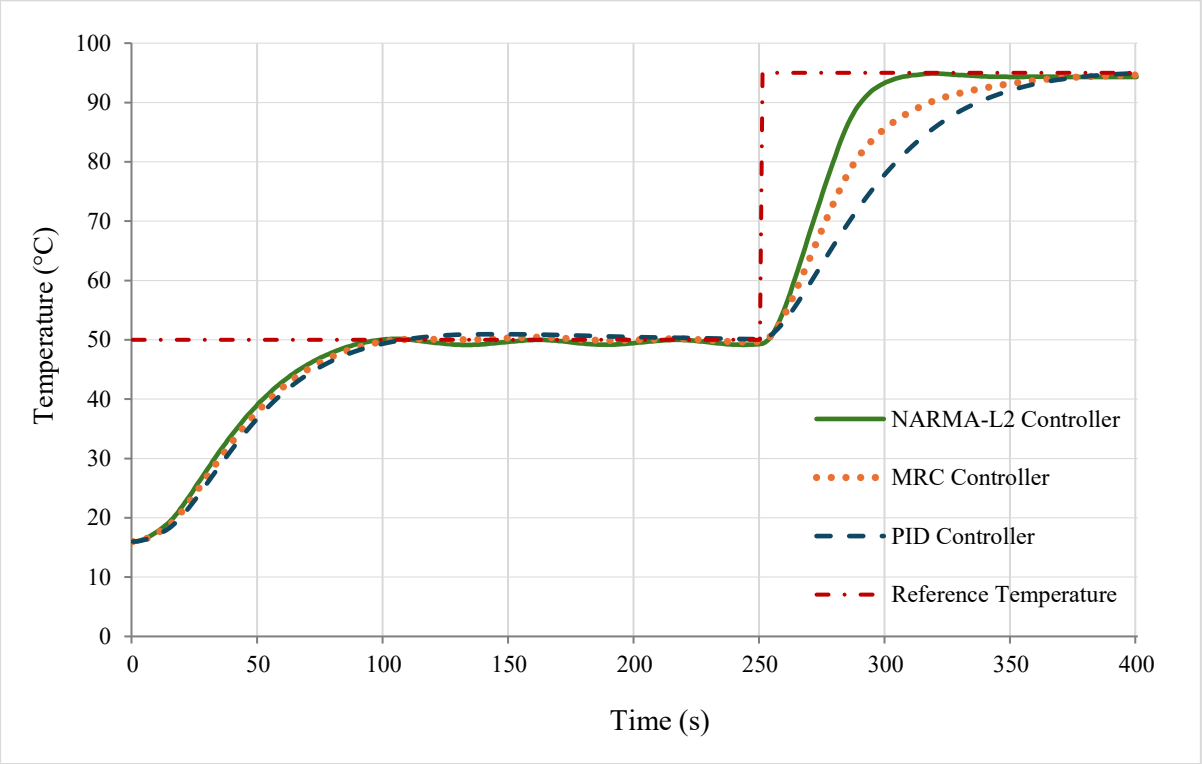


Fig. 23 Temperature response of NARMA-L2, MRC, and PID controller for a step change in input (50°C-95°C) with an initial conductivity of 0.60 S/m

Discussion on Sustainability Impacts

The carbon emission efficiency of the NARMA-L2, MRC, and PID controllers was evaluated based on their steady-state energy consumption during the 71–400 s operational period of the CFOH system. The quantity of greenhouse gas (GHG) emissions was determined utilising the UK power emission conversion factors for 2025 [25]. The emission conversion factors delineate GHG emissions per kWh of energy consumed, indicating a total emission intensity of 0.177 CO_2e kg/kWh, which includes 0.17489 kg CO_2/kWh, 0.00090 CH_4 kg/kWh, and 0.00122 N_2O kg/kWh. Assuming the system operates continuously, the energy consumption per steady-state cycle was extrapolated to yearly utilisation. The results indicate that the NARMA-L2 controller consistently exhibits the lowest emissions across all parameters. The MRC follows; however, the PID controller exhibits the highest emissions. This inclination is a direct consequence of the controllers' comparative energy efficiency. A decrease in steady-state energy demand results in a reduction of carbon intensity. The NARMA-L2-based controller emits approximately 8,083 kilos of CO_2e annually. The Model Reference controller emits 8,176 kilograms of CO_2e, whereas the PID controller emits 8,270 kilograms of CO_2e, as seen in Table 3. Although the differences in energy usage each cycle are negligible, prolonged operation of the machine significantly affects long-term greenhouse gas emissions. The PID controller generates approximately 184 kg more CO_2 annually compared to the NARMA-L2 controller. Similarly, emissions of CH_4 and N_2O remain small in absolute terms but

contribute to the total CO_2-equivalent footprint. These findings demonstrate that sophisticated neural network-based controllers not only enhance control performance but also offer tangible environmental benefits through improved energy efficiency.

To contextualise these results against conventional liquefied petroleum gas (LPG) heating methods. The heat transfer equation $Q = \dot{m} \cdot C_P \cdot \Delta T$ is employed to calculate the energy required to elevate the temperature using LPG heating. Where Q represents the heat duty in kW, $\dot{m}$ denotes the mass flow rate of the sauce (0.01767 kg/s, approximately 1 L/min), C_P denotes the specific heat capacity of the sauce (3.8 kJ/kg·°C), and ΔT indicates the temperature increase from 16°C to 95°C. The sauce absorbs a net thermal energy of E = 0.4847 kWh during the steady-state window.

Considering that industrial gas heating operates at approximately 75% efficiency [26], the required amount of LPG energy each cycle increases to 0.6463 kWh. Utilising UK emission figures for LPG (CO_2: 0.23032 kg/kWh, CH_4: 0.00020 kg/kWh, N_2O: 0.00012 kg/kWh) [25], The emissions per cycle amount to 0.1487 kg CO_2e. This totals 39.08 kg each day and 14,270 kg per year when the system operates continuously. LPG heating emits around 76% more greenhouse emissions annually compared to the contemporary NARMA-L2 controller. These results underscore the importance of integrating high-efficiency heating methods and energy-efficient control strategies to achieve substantial reductions in industrial carbon emissions

Table 3 The Comparison of greenhouse Gas (GHG) emissions from NARMA-L2, MRC, and PID controller-based CFOH heating with conventional LPG heating using UK power emission conversion coefficients for 2025

Controller	N_2O (kg/year)	CH_4 (kg/year)	CO_2 (kg/year)	Total CO_2e (kg/year)
NARMA-L2 (Ohmic)	55.66	41.06	7987	8083
MRC (Ohmic)	56.21	41.61	8078	8176
PID (Ohmic)	56.94	41.98	8171	8270
LPG heating	7.48	12.38	14270	14290

Future work

Future research will expand upon this comparative analysis by evaluating the proposed PID, MRC, and NARMA-L2 controllers in both real-time experimental and industrial-scale CFOH settings to address unmodeled dynamics, sensor noise, and actuator limitations. Future research will concentrate on enhancing the flexibility of neural network-based controllers through online learning, hybrid control architectures, and adaptive or self-tuning mechanisms to improve their robustness in response to variations in feedstock quality, environmental conditions, and load changes. Additionally, multi-objective optimisation frameworks including control performance, energy consumption, economic expenditure, and carbon emissions will be examined to assist individuals in making environmentally beneficial decisions. Subsequent research will examine the environmental impacts throughout the life cycle by employing dynamic emission variables and scenarios for the incorporation of renewable energy. This will improve long-term evaluations of sustainability. Finally, the scalability of smart controllers and their integration with digital twins, predictive maintenance techniques, and Industry 4.0-enabled monitoring systems will be examined to facilitate real-time optimisation and enhance their accessibility in sustainable thermal processing systems.

Conclusion

This study provided a comprehensive comparative analysis of NARMA-L2, Model Reference Control (MRC), and PID controllers for the precise temperature regulation of the CFOH system, highlighting dynamic performance metrics, energy efficiency, and sustainability objectives. The results unequivocally demonstrate that neural network-based controllers significantly outperform the conventional PID controller in both transient and steady-state operations. The NARMA-L2 controller exhibited the quickest rise time, the least transient and settling time, and no overshoot. This indicates enhanced responsiveness, less oscillation, and increased stability in closed-loop mode. The MRC exhibited commendable dynamic performance and acceptable overshoot during the entire operation, but the PID controller demonstrated much longer response times, the highest overshoot, and diminished stability. Despite NARMA-L2's increased energy usage during the transient phase due to its assertive control strategy, it exhibited the lowest steady-state power consumption and the highest efficiency. This indicated that it consumed less energy over time. When implemented on a daily and annual basis, it resulted in a reduction of greenhouse gas emissions. The NARMA-L2 controller exhibited the lowest annual CO_2e emissions, followed by the MRC controller, whereas the PID controller recorded the highest emissions. The results indicate that advanced neural network-based controllers enhance control accuracy and reliability while also benefiting the environment by reducing energy consumption and minimising carbon emissions. This renders them ideal for sustainable industrial thermal processes.

Author Contributions
T.J. and L.P.L. Writing - Original draft preparation; Methodology; Experimental setup; Data collection. W.I. Supervision. Validation; Writing-Review and Editing. J.S. Supervision; Validation; Writing-Review and editing. M.A. Supervision; Validation; Writing-Review and Editing. T.B. Supervision; Validation; Writing-Review and editing. C.M. Supervision; Validation; Writing-Review and Editing. M.R. Writing-Review and editing. H.Z. Supervision; Conceptualisation; Formal analysis; Resources; Writing-Review and editing. All authors have read and agreed to the published version of the manuscript.

Data Availability Statement
The raw data supporting the conclusions of this article will be made available by the authors on request.

Right Retention Statement
For the purpose of open access, the author has applied a Creative Commons Attribution (CC BY) licence to any Author Accepted Manuscript version arising from this submission.

Declarations

Informed Consent Statement Not applicable.

Competing Interests The authors declare no competing interests.

Acknowledgments
The authors would like to thank Premier Foods, Ohm-E Technology (UK), and the AFIC team at Sheffield Hallam University for their guidance and resources received during experiments.

Funding sources: This research was supported by Innovate UK under Grant number 10074002**.**

References

[1] Food and Drink Federation, “Industry at a glance,” *Business Insights and Economics*. [Online]. Available: https://www.fdf.org.uk/fdf/business-insights-and-economics/facts-and-stats/. [Accessed: Apr. 16, 2026]

[2] O. Corigliano, P. Morrone and A. Algieri, "Navigating the Challenges of Sustainability in the Food Processing Chain: Insights into Energy Interventions to Reduce Footprint," *Energies (Basel),* vol. 18, *(2),* pp. 296, 2025. . DOI: 10.3390/en18020296.

[3] B. L. Gowreesunker, S. Tassou and J. Atuonwu, "Cost-Energy Optimum Pathway for the UK Food Manufacturing Industry to Meet the UK National Emission Targets," *Energies (Basel),* vol. 11, *(10),* pp. 2630, 2018. . DOI: 10.3390/en11102630.

[4] O. Oluwole-ojo *et al*, "Energy Consumption Analysis of a Continuous Flow Ohmic Heater with Advanced Process Controls," *Energies (Basel),* vol. 16, *(2),* pp. 868, 2023. . DOI: 10.3390/en16020868.

[5] P. Richardson, *Thermal Technologies in Food Processing*. Cambridge, U.K.: Woodhead Publishing, 2001.

[6] V. J. Vandoren, "Open-loop control offers some advantages," *Control Eng.,* vol. 45, *(13),* pp. 176, 1998.

[7] R. Stirling, "Ohmic heating - a new process for the food industry," *Power Engineering Journal,* vol. 1, *(6),* pp. 365–371, 1987. . DOI: 10.1049/pe:19870065.

[8] P. J. Skudder and R. Stirling, "The commercial development of ohmic heating processes," in *IEE Colloquium on Advanced Food Technology,* 1992, .

[9] J. Li and F. Li, "Active control of thermal buckling for plates using a temperature feedback control method," *Smart Mater. Struct.,* vol. 28, *(4),* pp. 045001, 2019. .

[10] D. Çelik *et al*, "Advancements in nonlinear PID controllers: A comprehensive review," *Comput. Electr. Eng.,* vol. 129, pp. 110775, 2026. . DOI: 10.1016/j.compeleceng.2025.110775.

[11] B. Dinç and K. Erentürk, "Comparison of PID and FLC type controller designed for ohmic heating system," in *SETSCI-Conference Proceedings,* 2024, .

[12] Z. Dong *et al*, "Fuzzy temperature control of induction cooker," in *IECON 2017-43rd Annual Conference of the IEEE Industrial Electronics Society,* 2017, .

[13] T. Alamirew, V. Balaji and N. Gabbeye, "Design of model predictive controller for pasteurization process," *Indonesian Journal of Electrical Engineering and Informatics (IJEEI),* vol. 5, *(2),* pp. 137–144, 2017. .

[14] J. Zhang and M. Wang, "Special Issue: Neural Networks, Fuzzy Systems and Other Computational Intelligence Techniques for Advanced Process Control," *Processes,* vol. 11, *(8),* pp. 2278, 2023. . DOI: 10.3390/pr11082278.

[15] I. O. Bachi, A. S. Bahedh and I. A. Kheioon, "Design of control system for steel strip-rolling mill using NARMA-L2," *J Mech Sci Technol,* vol. 35, *(4),* pp. 1429–1436, 2021. . DOI: 10.1007/s12206-021-0308-7.

[16] H. E. Elfadel Haroon, "Nonlinear auto-regressive moving average (NARMA-L2) controller design for two CSTR," in *2024 10th International Conference on Electrical Engineering, Control and Robotics (EECR),* 2024, . DOI: 10.1109/EECR60807.2024.10607333.

[17] R. Paul and S. Chokkadi, "Implementation of NARMA-L2 Controller for Shell and Tube Heat Exchanger Temperature Process," *Ind Eng Chem Res,* vol. 55, *(19),* pp. 5644–5653, 2016. . DOI: 10.1021/acs.iecr.5b03791.

[18] W. Uddin *et al*, "A Neural Network-Based Model Reference Control Architecture for Oscillation Damping in Interconnected Power Systems," *Energies (Basel),* vol. 12, *(19),* pp. 3653, 2019. . DOI: 10.3390/en12193653.

[19] O. Oluwole-ojo *et al*, "Model Validation and Real-Time Process Control of a Continuous Flow Ohmic Heater," *Modelling,* vol. 5, *(3),* pp. 752–775, 2024. . DOI: 10.3390/modelling5030040.

[20] MathWorks, "Design NARMA-L2 Neural Controller in Simulink," *MATLAB & Simulink Documentation*. [Online]. Available: Design NARMA-L2 Neural Controller in Simulink. [Accessed: Apr. 16, 2026].

[21] K. S. Narendra and K. Parthasarathy, "Learning automata approach to hierarchical multiobjective analysis," *IEEE Trans. Syst. Man Cybern.,* vol. 21, *(1),* pp. 263–272, 2002. .

[22] M. T. Hagan et al, "Training recurrent networks for filtering and control," Recurrent Neural Networks: Design and Applications, pp. 311–340, 1999. .

[23] K. S. Narendra and S. Mukhopadhyay, "Adaptive control using neural networks and approximate models," IEEE Trans. Neural Networks, vol. 8, (3), pp. 475–485, 1997. .

[24] T. Javed et al, "Integrating fluid dynamics: leveraging Simscape for modelling and real-time control of continuous flow ohmic heater," International Journal of Modelling and Simulation, pp. 1–16, 2025. .

[25]" Department for Energy Security and Net Zero, "Greenhouse gas reporting: conversion factors 2025," U.K. Government, Jun. 10, 2025. [Online]. Available: https://www.gov.uk/government/publications/greenhouse-gas-reporting-conversion-factors-2025. [Accessed: Apr. 16, 2026].

[26] B. S. Fakinle et al, "Emission characterization and performance of conventional liquefied petroleum gas cookstove burners," Cogent Engineering, vol. 6, (1), pp. 1652228, 2019.